

Analysis of a Heat Pipe Assisted Heat Sink

John Thayer
Thermacore International
780 Eden Road
Lancaster, PA 17604-3234
Tel: 717-569-6551 x208
John.Thayer@Thermacore.com

Introduction

Heat pipes can be useful in improving the performance of heat sinks in electronics cooling applications. As phase change heat transfer devices, heat pipes very effectively transfer heat over their length with only a small temperature gradient. Heat pipes are commonly available in two form factors; cylindrical heat pipes that transfer heat in 1 dimension, and vapor chambers (flat heat pipes) that transfer heat in 2 dimensions. When used in high heat flux applications where conduction losses are significant, heat pipes can reduce component temperatures by 10-20C.

This paper reports on the analytical and experimental results of such an application. A heat sink for a high power forced convection telecom cooling application was optimized using Flotherm CFD modeling. Three design options were considered; plain aluminum base, an aluminum base with 3 cylindrical heat pipes embedded in machined grooves, and a vapor chamber base. All options used the same folded fin stack. The Flotherm analysis accurately predicted the benefit of using heat pipes for minimizing spreading resistance in the base of the heat sink. Table 1 gives the comparison between analytical and experimental results.

Table 1

Heat Sink Design	Θ_{HS-A} (C/W)		
	Model	Test	Ratio
Plain Base	0.39	0.36	110%
Embedded Heat Pipe	0.30	0.29	103%
Vapor Chamber	0.24	0.24	103%

Description of the Heat Sink

The heat sink had a base of 150 mm in the flow direction and 215 mm across the flow. The base was 8 mm thick. The fin stack was folded fin of 0.6 mm thickness, 1.6 mm pitch, and 18 mm height. The fins extended only 76 mm in length, covering less than half the base length. The base was alloy 6063 and the fins were alloy 1100. The fins and base were nickel plated and soldered together.

Two heat sources, listed in Table 2, were bolted to the base, with a layer of thermal interface material in between.

Table 2

Heat Source	Size (mm)	Power (W)	Flux (W/cm ²)
Major	25 x 9.5	84	35
Minor	19 x 6.4	11	9

The design airflow was 30 m³/hr at 30 Pa pressure drop. The heat sink is intended to be mounted on a circuit board and installed in a card cage at a 30 mm board pitch.

Initial calculations showed that spreading resistance in the base was the dominant portion of the overall thermal resistance, 20 C out of an estimated total of 35 C. Thus the heat sink was an excellent candidate for heat pipe augmentation. As mentioned, 3 designs were under consideration; plain aluminum base, an aluminum base with 3 cylindrical heat pipes embedded in machined grooves, and a vapor chamber base. The embedded heat pipes were 0.25" diameter copper/water heat pipes of varying lengths, formed into curved shapes that fit within the restricted areas of the heat sink base but extended to spread the heat to the far corners of the sink. The pipes were pressed into round bottom grooves and flattened on top to be coplanar with the base surface. They were soldered in place. The copper vapor chamber was mounted in an aluminum frame and extended to the area underneath the fin. Figures 1 and 2 show top and bottom views of the heat sink.



Figure 1 – Heat Sink fin stack

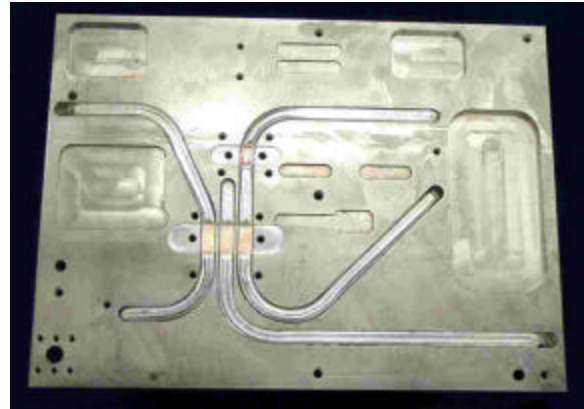


Figure 2 – Heat Sink Base with Embedded Heat Pipes

Flotherm Model

To evaluate the performance gain available from a heat pipe heat sink design, Flotherm models were constructed of all 3 designs. In general heat pipes can be modeled with 4 elements:

- Copper walls
 - + Cuboid with the external dimension of heat pipe.
 - + $k = 380 \text{ W/mK}$
- Vapor space
 - + Cuboid with the internal dimension of the hollow space.
 - + $k = 50000 \text{ W/mK}$
- Wick
 - + Collapsed cuboid at the interface between the Cu wall and the vapor space & thickness of 1 mm
 - + $k = 40 \text{ W/mK}$
- Interface
 - + Collapsed cuboid at the interface between the Cu wall and the surrounding solid & thickness of the interface material.
 - + $k = \text{appropriate for contact resistance.}$

This modeling scheme captures the main aspects of heat pipe heat transfer. In particular the high conductivity vapor space allows heat to flow with virtually no temperature gradient along the entire length of the heat pipe. It captures the wick resistance as the primary component of overall thermal resistance of the heat pipe itself. It allows the possibility of spreading in the copper walls. And any thermal interface between the heat pipe and other model elements can be included.

While vapor chambers often have significant spreading in their walls, embedded heat pipes usually have negligible lateral spreading. There is little to be gained by making the walls cuboid elements with 3 dimensional conduction. The modeling scheme was simplified for the embedded heat pipe model by lumping the copper wall, wick and interface into one collapsed cuboid element with 1 dimensional heat flow. The effective conductivity would represent the resistance to heat flow of all three layers. This also has the beneficial effect of eliminating very thin cells required to represent the walls.

- Copper walls, wick & interface.
 - + Envelope of collapsed cuboids with the external dimension of the heat pipe.
 - + k = effective for 3 layers (usually dominated by the interface)
- Vapor space
 - + Cuboid with the external dimension of the heat pipe.
 - + $k = 50000 \text{ W/mK}$

It is important to note that this modeling scheme does NOT model the physics of phase change heat transfer. Artifices are used to represent two major factors

in heat pipe heat transfer. While conduction in a super high conductivity cuboid may have low gradients, it does not model vapor flow, the associated pressure gradient and consequent temperature gradient. The temperature gradient associated with the boiling of fluid at the heat source is only represented in a coarse fashion as a constant conductive resistance of a collapsed cuboid. None of the nuances such as dependence on heat flux, wick structure, etc., are captured. The value of conductivity for the wick of 40 W/mK is a conservative value suitable for typical sintered copper powder wicks and relatively low heat fluxes of below 50 W/cm^2 .

It is also important to note that this modeling scheme does NOT model the real limits to maximum heat flow imposed by such factors as viscous losses in the return flow of condensate in the wick. It is quite possible to analytically achieve unrealistically high heat flow in such a model. A complete heat pipe design analysis would include a separate evaluation of the maximum power capability.

Because all three base designs used the same fin stack, the airflow side of the Flotherm model needed to be solved only once. Since this was the most time consuming part of the number crunching, this tactic was used. To facilitate this all the heat pipe model elements were included in the same overall model (thus using the same grid and hence same flow field). For the thermal solution the appropriate heat pipe elements were turned on or off and a "Freeze Flow" thermal solution was recomputed for each different design.

Figures 3, 4 & 5 show the geometry of the heat sink and heat pipe model.

Figure 3 - Heat Sink Outline

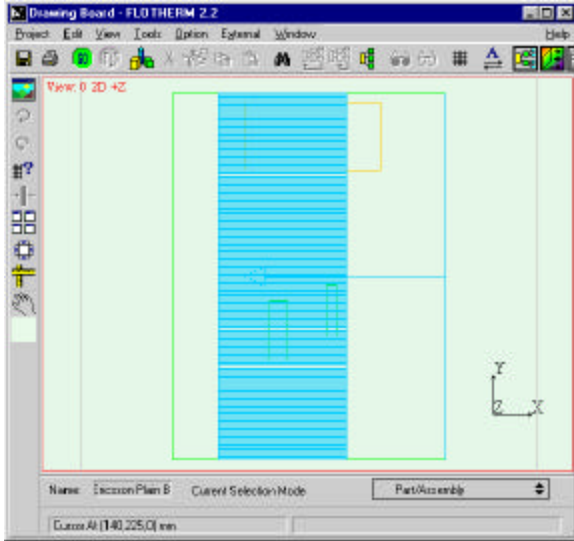


Figure 4 - Embedded Heat Pipe Layout

(Note that the Flotherm analysis and matching experimental data was of an earlier design rev than that shown in the photo of Figure 2)

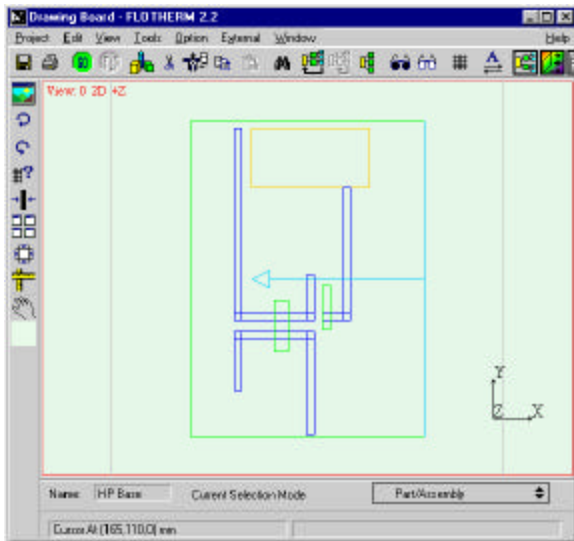
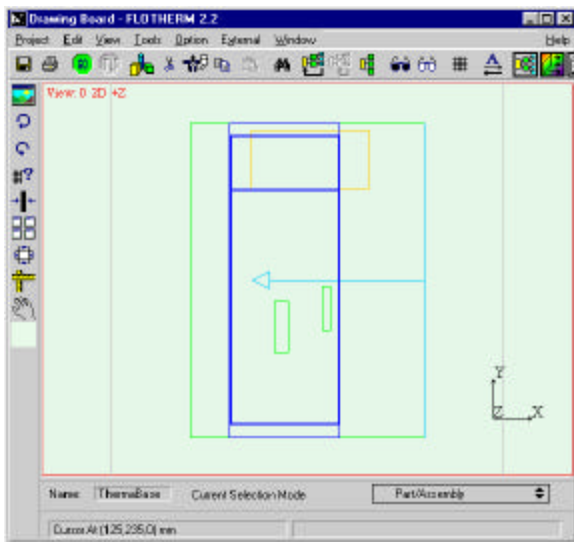


Figure 5 - Vapor Chamber Layout



Results

Figure 6 - Plain Base Results
Temperature Contours

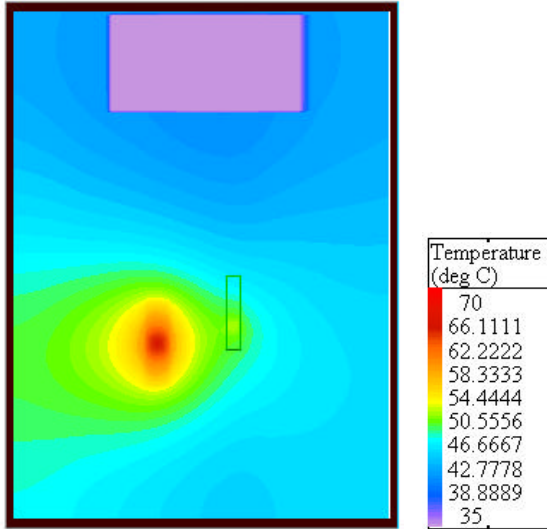


Figure 7 - Embedded Heat Pipe Results
Temperature Contours

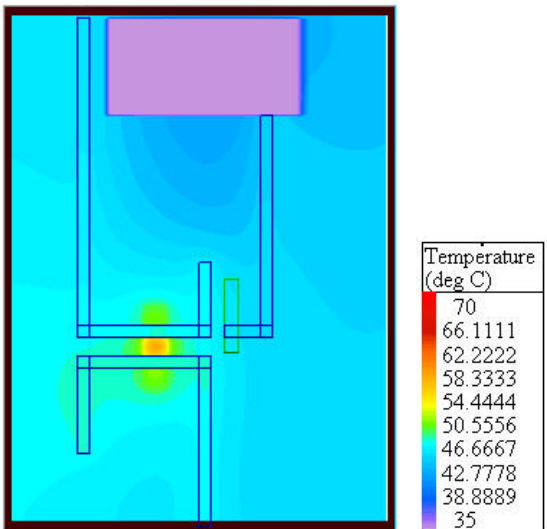
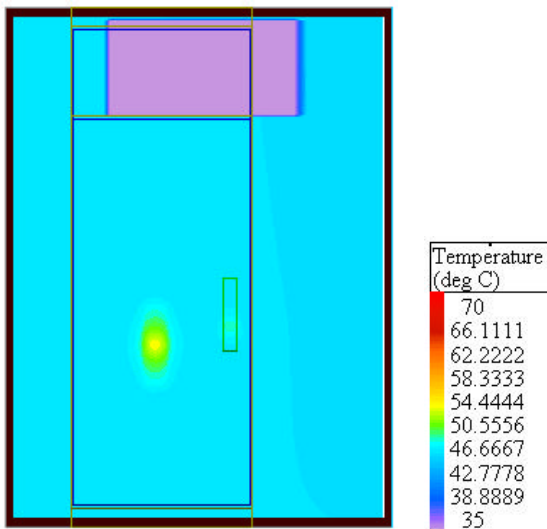


Figure 8 - Vapor Chamber Results
Temperature Contours



The Flotherm results predicted a 23% improvement in heat sink thermal resistance for the embedded heat pipe version and a 38% improvement for the vapor chamber version. Based on these predictions it was deemed that sufficient gain was available to warrant the fabrication of prototype heat sinks.

The prototypes were tested in a channel flow test fixture that matched the dimensions and flow conditions of the card cage. There was an excellent match between the Flotherm results and experimental data, as shown in Table 1 and Chart 3.

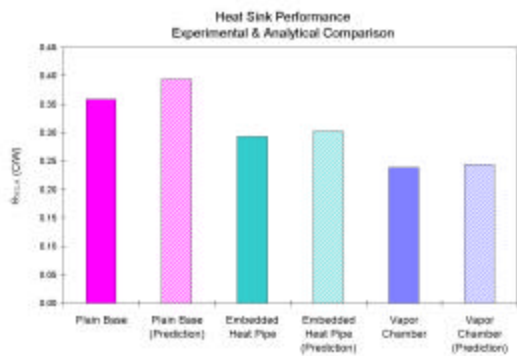


Chart 3 – Experimental & Analytical Results Comparison

For the current power level of 84 W, the heat pipe and vapor chamber designs offered 5.5 C and 10 C component temperature reductions respectively. As the power dissipation for the design rises to the expected 150 W level, the improvement will be on the order of 20 C, making the heat pipe a make-or-break cooling technology for this design.

Experimental error is on the order of +/- 10%, due primarily to thermocouple error and parasitic power loss from the

heater. Analytical error is on the order of +/- 20%, primarily due to the simplification used for modeling wick resistance. Chart 4 shows with experimental data that rather than being a constant value, as assumed, heat sink resistance varies with power (due to wick resistance heat flux dependency). Unfortunately Flotherm cannot vary material conductivity (the modeling mechanism for wick resistance) by heat flux. In addition, there are the usual CFD error sources, primarily grid refinement near the heat source and in the boundary layer of the fins. Because of the large number of fins, only a coarse grid of 2 cells between each fin could be solved. Even still the total grid size was 590000 cells.

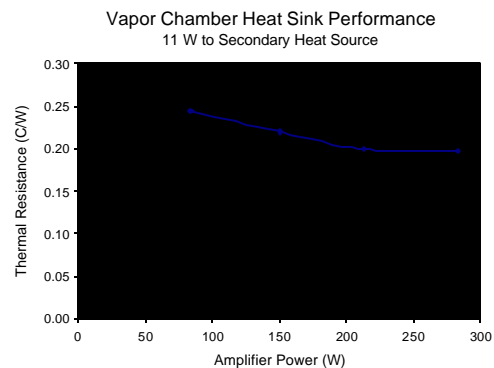


Chart 4 – Heat Sink Resistance vs Power

Conclusion

The heat transfer effects of heat pipes in electronic cooling applications can be modeled with reasonable accuracy in Flotherm. This allows the thermal engineer to assess the potential benefit of adding heat pipes to a design in a timely and cost efficient manner. This would include early stage feasibility studies as well as design optimization in a later, prototype design stage.